Center of Ventilation—Methods of Calculation using Electrical Impedance Tomography and the Influence of Image Segmentation

V. Sobota[1] and K. Roubik[1]

[1] Faculty of Biomedical Engineering, Czech Technical University in Prague, Kladno, Czech Republic

Abstract— **Electrical impedance tomography (EIT) is a promising non-invasive, radiation-free imaging modality. Using EIT-derived index Center of Ventilation (CoV), ventral-to-dorsal shifts in distribution of lung ventilation can be assessed. The methods of CoV calculation differ among authors and so does the segmentation of EIT images from which the CoV is calculated. The aim of this study is to compare the values of CoV obtained using different algorithms, applied in variously segmented EIT images. An animal trial (n=4) with anesthetized mechanically ventilated pigs was conducted. In one animal, acute respiratory distress syndrome (ARDS) was induced by repeated whole lung lavage. Incremental steps in positive end-expiratory pressure (PEEP), each with a value of 5 cmH$_2$O (or 4 cmH$_2$O in the ARDS model), were performed to reach total PEEP level of 25 cmH$_2$O (or 22 cmH$_2$O in the ARDS model). EIT data were acquired continuously during this PEEP trial. From each PEEP level, 30 tidal variation (TV) images were used for analysis. Functional regions of interest (ROI) were defined based on the standard deviation (SD) of pixel values, using threshold 15%–35% of maximum pixel SD. The results of this study show that there might be statistically significant differences between the values obtained using different methods for calculation of CoV. The differences occured in healthy animals as well as in the ARDS model. Both investigated algorithms are relatively insensitive to the image segmentation.**

Keywords— **center of ventilation, center of gravity, electrical impedance tomography, EIT, region of interest**

I. Introduction

Electrical impedance tomography (EIT) is an imaging modality that provides information about regional lung ventilation. It is based on the application of small alternating currents using skin electrodes attached to the patient's chest and the consequent measurement of resulting voltages. It can offer a non-invasive, radiation-free bedside alternative to computed tomography in monitoring of tidal volume (V_T) distribution and lung aeration inhomogeneity [1].

Due to the physical principle used, EIT images suffer from low spatial resolution [2], [3] and the information provided by EIT is rather complex and may be difficult to interpret [3]. Therefore, several indices and measures were developed to assess lung ventilation [4].

One of the most widely used indices in EIT data processing is called Center of Ventilation (CoV) and was introduced for the first time in 1998 by Frerichs et al. [5]. It describes shifts in distribution of lung ventilation in ventral-to-dorsal direction. In that study, it was defined as a weighted mean of geometrical centers of the right and the left lung. In 2006, the same research group presented a modified approach for its calculation where CoV was calculated separately for both left and right lung [6].

Since CoV has proven to be a useful index in assessment of regional lung ventilation, it was adopted by many research groups [7]–[12]. However, the definitions of CoV are not consistent among these studies. Some authors define CoV as a weighted mean of the row sums [7], [9], [11], [12]. Van Heerde et al. defined CoV as "the point where the sum of fractional ventilation was 50% of the summed fractional ventilation" [8] and Blankman et al. computed it as a ratio between dorsal and total fractional ventilation [10]. Similarly to CoV, Center of Gravity (CoG) index was introduced in 2007 as a weighted mean of image row sums [13].

Unfortunately, different definitions of CoV are not the only inconsistency in its use. Segmentation of EIT images from which the CoV is calculated also varies. Initially, circular mask was applied to the EIT image and the resulting area was divided into several regions of interest (ROI) [6], [8]. However, some authors use functional segmentation of the images, defined as 20% of maximum regression coefficient obtained between global and local relative impedance [11] or as 20% of the maximum standard deviation (SD) of the pixel value in certain time period [12]. Finally, there are studies where CoV was calculated without any previous image segmentation [9].

As there are different definitions of CoV published, used together with various EIT image segmentation, we hypothesized that the resulting CoV values and thus the evaluation of regional lung ventilation may differ.

The aim of this study is to compare the values of CoV obtained using different methods of its computation, applied in variously segmented images.

Sobota, V. and Roubik, K., 2016. Center of Ventilation—Methods of Calculation Using Electrical Impedance Tomography and the Influence of Image Segmentation. In *XIV Mediterranean Conference on Medical and Biological Engineering and Computing 2016* (pp. 1258-1269). Springer, Cham.

II. METHODS

The study protocol was approved by the Institutional Review Board of the First Faculty of Medicine, Charles University in Prague (FFM CU) and is in accordance with Act No. 246/1992 Coll., on the protection of animals against cruelty. The measurements were performed at an accredited animal laboratory of the FFM CU.

Four crossbred Landrace female pigs (*Sus scrofa domestica*) with a body weight of 48 ± 2 kg were used in this study.

A. Anesthesia and preparation

The animals were premedicated with azaperone (2 mg/kg IM). Anesthesia was initiated with ketamine hydrochloride (20 mg/kg IM) and atropine sulphate (0.02 mg/kg IM), followed by boluses of morphine (0.1 mg/kg IV) and propofol (2 mg/kg IV). A cuffed endotracheal tube (I.D. 7.5 mm) was used for intubation. Anesthesia was maintained with propofol (8 to 10 mg/kg/h IV) in combination with morphine (0.1 mg/kg/h IV) and heparin (40 U/kg/h IV). To suppress spontaneous breathing, myorelaxant pipecuronium bromide (4 mg boluses every 45 min) was administered during mechanical lung ventilation. Initially, rapid infusion of 1 000 mL of saline was administered intravenously, followed by a continuous IV administration of 250 mL/h to reach and maintain central venous pressure of 6 to 7 mmHg.

Mixed venous blood oxygen saturation and continuous cardiac output were measured by Vigilance (Edwards Lifesciences, Irvine, CA, USA) monitor. Arterial blood gases, i.e. arterial partial pressure of oxygen, carbon dioxide ($PaCO_2$) and pH, were continuously measured by CDI 500 (Terumo, Tokyo, Japan). The arterio-venous extracorporeal circuit for CDI 500 monitor was established between the femoral artery and the femoral vein using a mechanical blood pump (peristaltic roller pump with a blood flow set to 400 mL/min).

In one animal, repeated whole lung lavage (normal saline, 30−40 mL/kg, 37°C) was performed to induce the surfactant deficiency similar to acute respiratory distress syndrome (ARDS) [8].

B. Ventilation

Conventional ventilator Hamilton G5 (Hamilton Medical AG, Bonaduz, Switzerland) was used in the CMV mode with the following setting: respiratory rate 18 bpm, FiO_2 21%, I:E 1:2 with initial positive end-expiratory pressure (PEEP) of 5 cmH_2O and pressure limit set to 40 cmH_2O. The initial V_T was set to 8.5 mL/kg of the actual body weight and was titrated to reach normocapnia ($PaCO_2$ 40 ± 3 mmHg). During the study protocol four increasing PEEP steps of 5 cmH_2O were performed in animals with healthy lungs and three increasing PEEP steps of 4 cmH_2O with initial value of 10 cmH_2O were performed in the ARDS model. Each PEEP level was maintained at least for 3 minutes.

C. EIT measurements

EIT system PulmoVista 500 (Dräger Medical, Lübeck, Germany) was used for data acquisition. The electrode belt (size S) was attached to the chest of the animal at the level of the 6^{th} intercostal space. The frequency of the applied current was set to 110 kHz with amplitude of 9 mA. EIT images were recorded continuously with a frame rate of 50 Hz during the entire PEEP maneuver.

D. Data Processing

The acquired data were pre-processed in Dräger EIT Data Analysis Tool 6.1 (Dräger Medical, Lübeck, Germany). Baseline frame was set automatically for each animal as a frame that corresponds with the global minimum of impedance waveform. Reconstructed data were processed in MATLAB 2014b (MathWorks, Natick, MA, USA).

At each PEEP level, EIT data from 30 consecutive breaths were used for analysis. The breaths were selected in the phases where the values of end-expiratory lung impedance were the most stable. Tidal variation (TV) images were calculated as a difference between end-inspiratory and end-expiratory EIT images. In consequence, 30 TV images were obtained for each PEEP level.

Functional ROI was defined based on the standard deviation (SD) of individual pixel values in time [12], [14]. Six threshold levels ranging from 15% to 40% of maximum pixel SD with 5% step were used for image segmentation. For each set of 30 TV images, a common ROI was applied. The index called Center of Gravity (CoG) was defined as a weighted mean of row sums obtained from TV image [13]:

$$\mathrm{CoG} = \frac{1}{N+1} \cdot \frac{\sum_{x=1}^{N} \sum_{y=1}^{N} y \cdot TV_{xy}}{\sum_{x=1}^{N} \sum_{y=1}^{N} TV_{xy}} \qquad (1)$$

where N stands for both the number of pixel rows and pixel columns in the TV image ($N = 32$ for EIT images provided by PulmoVista 500) and TV_{xy} stands for the value of the pixel with coordinates x,y.

For the purposes of this study, Center of Ventilation (CoV) index was defined as a vertical coordinate that divides the sum of fractional ventilation in two equal halves [8] (Fig. 1). Our implementation of the algorithm for calculation of CoV can be summarized as follows:

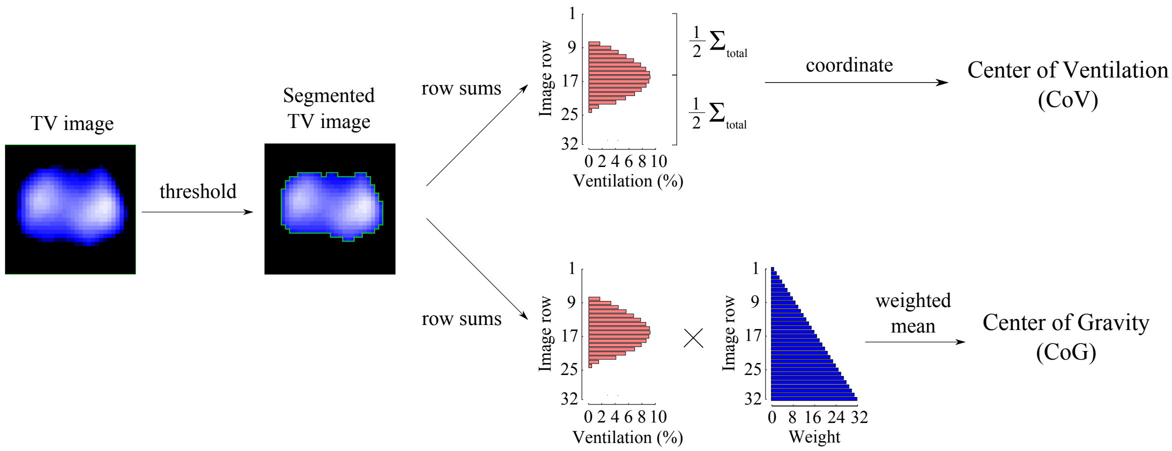

Fig. 1: Computation of Center of Ventilation (CoV) and Center of Gravity (CoG). Tidal variation (TV) images were segmented and a region of interest (ROI) was defined. Row sums were calculated from the segmented TV image. CoV was calculated as a coordinate that divides row sums in two equal halves. CoG was calculated as a weighted mean of image row sums.

1. Normalize the pixel values in the TV image:

$$TV^*_{xy} = \frac{TV_{xy}}{\sum_{x=1}^{N}\sum_{y=1}^{N} TV_{xy}} \cdot 100 \tag{2}$$

   where TV^*_{xy} expresses the value of the original pixel TV_{xy} as a percentage of the total sum of the TV image.
2. Calculate row sums of the normalized TV image and save them into the array $\mathbf{r}$.
3. Find the highest index $n \in \mathbb{N}$ for which holds:

$$\sum_{i=1}^{n} \mathbf{r}_i \leq 50 \tag{3}$$

4. Calculate the ratio k:

$$k = \frac{50 - \sum_{i=1}^{n} \mathbf{r}_i}{r_n} \tag{4}$$

5. Calculate the value of CoV:

$$\text{CoV} = \frac{n + k + 0.5}{N + 1} \tag{5}$$

For calculation of both CoV and CoG, a coordinate system with the top left pixel represented by coordinates $x = 1$, $y = 1$ was used. In the following text the abbreviations "CoV" and "CoG" refer to the indices described above and the unabbreviated term "Center of Ventilation" represents the index in general.

Paired two-tailed t-test was used for evaluation of statistical differences between CoV and CoG. The values of both indices obtained at different PEEP levels were visualized as a box plot.

III. Results

EIT data from 4 animals were studied. The highest PEEP step was omitted in two subjects due to their hemodynamic instability. In total 510 TV images were analyzed.

In general, the values of CoV were significantly higher ($p<0.05$) than the corresponding values of CoG in all subjects. As shown in Table 1, there were four cases where the difference between CoV and CoG was not statistically significant and three cases where the mean value of CoG was higher than the corresponding mean value of CoV.

Box plots were created for each animal to visualize the effect of image segmentation upon values of both CoV and CoG. Figure 2 shows typical values of these indices during incremental PEEP steps. Both CoV and CoG move dorsally when a higher PEEP level is applied. When calculated from segmented TV images, variation in values of both indices decreases with higher threshold.

The effect of image segmentation upon the values of CoV and CoG is rather small when the indices are calculated from mean TV image, as illustrated in Fig. 3 and 4. The influence of PEEP upon both indices is much higher when compared to the changes caused by application of different image segmentation thresholds.

IV. Discussion

The results of this study show, that in general, there is a statistically significant difference between the values obtained using different methods for calculation of Center of Ventilation. Both presented algorithms for its calculation show relatively low sensitivity to lung segmentation.

Table 1: The differences CoV−CoG (mean ± SD). Statistically insignificant differences (paired t-test, $p > 0.05$) are marked as *. The cases where the mean value of CoG is higher than the value of CoV are marked as †. Repeated whole lung lavage was performed in pig 4.

Pig	PEEP level	Threshold (% of max. SD)					
	(cmH_2O)	15	20	25	30	35	40
1	5	0.290 ± 0.049	0.315 ± 0.043	0.361 ± 0.045	0.392 ± 0.053	0.509 ± 0.047	0.509 ± 0.040
	10	0.477 ± 0.089	0.434 ± 0.046	0.387 ± 0.028	0.383 ± 0.057	0.308 ± 0.048	0.308 ± 0.043
	15	0.348 ± 0.112	0.193 ± 0.058	0.166 ± 0.012	0.191 ± 0.027	0.090 ± 0.027	0.090 ± 0.027
	20	0.507 ± 0.333	$0.034 \pm 0.179^{*}$	0.062 ± 0.054	0.098 ± 0.036	0.047 ± 0.036	0.047 ± 0.031
	25	1.131 ± 0.434	0.539 ± 0.374	$0.088 \pm 0.243^{*}$	0.066 ± 0.093	0.057 ± 0.051	0.057 ± 0.049
2	5	0.770 ± 0.122	0.823 ± 0.112	0.908 ± 0.110	0.845 ± 0.101	0.719 ± 0.091	0.719 ± 0.086
	10	1.158 ± 0.063	1.174 ± 0.054	0.972 ± 0.050	0.635 ± 0.056	0.513 ± 0.055	0.513 ± 0.044
	15	0.851 ± 0.056	0.314 ± 0.023	0.186 ± 0.026	0.138 ± 0.025	0.080 ± 0.021	0.080 ± 0.019
	20	0.507 ± 0.017	0.093 ± 0.026	0.026 ± 0.028	$-0.001 \pm 0.030^{\dagger *}$	$-0.039 \pm 0.029^{\dagger}$	$-0.039 \pm 0.033^{\dagger}$
3	5	0.193 ± 0.122	0.186 ± 0.121	0.181 ± 0.118	0.186 ± 0.117	0.052 ± 0.122	$0.052 \pm 0.110^{*}$
	10	0.498 ± 0.098	0.448 ± 0.098	0.407 ± 0.103	0.355 ± 0.105	0.221 ± 0.107	0.221 ± 0.102
	15	0.647 ± 0.106	0.532 ± 0.063	0.358 ± 0.050	0.320 ± 0.055	0.198 ± 0.057	0.198 ± 0.059
	20	0.460 ± 0.233	0.307 ± 0.159	0.246 ± 0.067	0.240 ± 0.040	0.146 ± 0.041	0.146 ± 0.036
4	10	0.304 ± 0.206	0.351 ± 0.199	0.234 ± 0.129	0.166 ± 0.078	0.106 ± 0.081	0.106 ± 0.084
	14	0.528 ± 0.255	0.497 ± 0.231	0.385 ± 0.176	0.341 ± 0.138	0.264 ± 0.127	0.264 ± 0.113
	18	1.116 ± 0.474	1.088 ± 0.479	0.930 ± 0.448	0.730 ± 0.392	0.449 ± 0.312	0.449 ± 0.237
	22	1.338 ± 0.376	1.197 ± 0.387	1.051 ± 0.380	0.742 ± 0.324	0.311 ± 0.220	0.311 ± 0.134

Although statistically significant, the differences between the values of CoV and CoG presented in this study are mostly at the edge of clinical relevance or even negligible. However, as shown in Fig. 5, there might be considerable differences in some subjects.

When functional ROI is applied to TV image, the variation in values of both CoV and CoG and the difference between their mean values decrease with an increasing threshold of lung segmentation. This is mainly due to the fact that the pixels with low change of relative impedance in time represent poorly ventilated lung regions or tissues that does not participate in ventilation at all. When these pixels are excluded from the ROI, only the lung regions that substantially contribute to ventilation are used for the calculation. In consequence, this may result in cases where CoV and CoG switch their positions when a high segmentation threshold is applied, as shown in Table 1. Similarly, the mean difference between CoV and CoG values substantially decreases when large insufficiently ventilated lung regions are omitted from the calculation because of the use of high segmentation threshold, as shown in the values of the ARDS model in Table 1.

Contrary to the effect of lung segmentation, when incremental PEEP steps are performed, the lung area that is predominantly ventilated moves dorsally. Therefore, the changes of both CoV and CoG values caused by PEEP setting are more pronounced.

For the purposes of this study we expressed both CoV and CoG in percentage as we consider this as the most common way [6]–[9], [12]. However, the expression as a value from the interval $\langle 1, N \rangle$, where N stands for the number of image row is also possible and correct [13].

To enable the comparison of two different approaches for calculation of Center of Ventilation, we modified the published algorithms to provide the value of 50% for a homogeneous image and also for images that are symmetrical along vertical axis. Both algorithms are also shift invariant for the structures that are symmetrical along vertical axis (top row of Fig. 5). Therefore, the biggest differences between CoV and CoG occur for the images with a strong horizontal asymmetry as shown in the bottom row of Fig. 5.

We used the abbreviation "CoV" for the method presented by van Heerde et al. [8] as it is in our opinion closer to the original idea of geometrical center of ventilation [5], [6]. The methods for calculation of this index presented in [7], [9], [11], [12] are closer to the idea of Center of Gravity index [13]. Therefore, abbreviation "CoG" was used for this

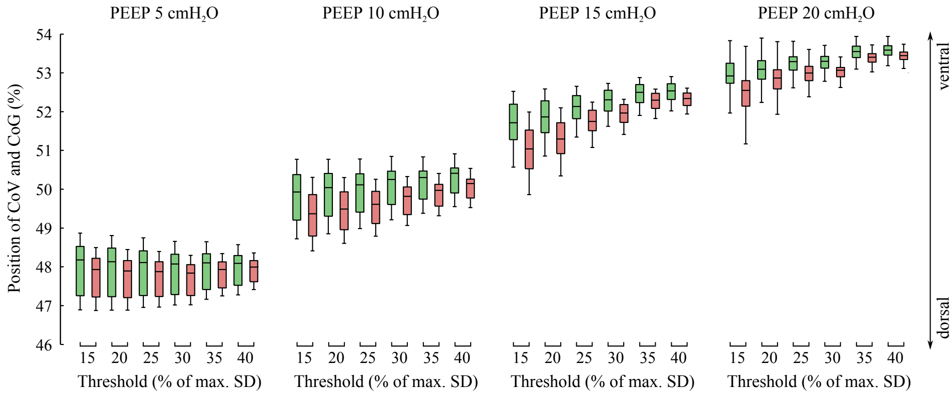

Fig. 2: Values of Center of Ventilation (red) and Center of Gravity (green) calculated from EIT images that were segmented using thresholds in the range of 15% – 40% of maximum pixel standard deviation (SD). The data obtained at four different PEEP levels are presented as box-and-whisker plot (minimum – lower quartile – median – upper quartile – maximum).

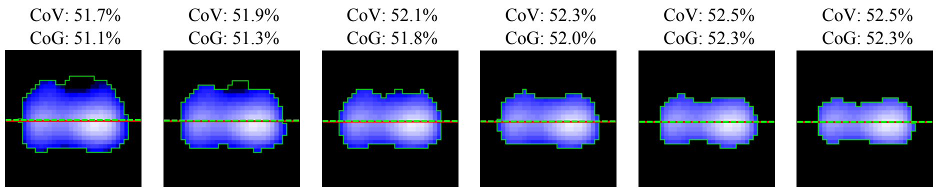

Fig. 3: Thresholding effect upon mean tidal variation (TV) image in the range from 15% to 40% in 5% steps (pig 3, PEEP 15 cmH$_2$O). The position of Center of Ventilation (CoV) and Center of Gravity (CoG) is depicted with red solid line and green dashed line, respectively. The pixel values of the image were obtained as a mean of 30 consecutive TV images.

method. In this study we did not evaluate the method presented by Blankman et al. [10].

Segmentation of TV images based on SD values of individual pixels is one of the most common approaches used for definition of functional ROI [14]. For this method, there is a recommended range of threshold values from 20% to 35% of maximum pixel SD. In this study we used threshold values ranging from 15% to 40% to assess also the effect of ROIs that are produced by setting of the threshold criteria outside the recommended range.

V. Conclusion

This study shows that there is a statistically significant difference between the values provided by the two studied methods for calculation of Center of Ventilation. The differences occured in healthy animals as well as in the model of lung injury. In consequence, assessment of ventral-to-dorsal shifts in lung ventilation may be compromised. However, both algorithms that were evaluated are relatively insensitive to the segmentation of EIT images.

Acknowledgements

The authors thank the employees of the animal laboratory of the Department of Physiology, FFM CU, where the animal trial was performed. The study was supported by grants VG20102015062 and SGS14/216/OHK4/3T/17.

The authors declare that they have no conflict of interest.

References

1. Frerichs I., Hinz J., Herrmann P., et al. Detection of local lung air content by electrical impedance tomography compared with electron beam CT *J Appl Physiol.* 2002;93:660-666.
2. Holder D.S.. *Electrical Impedance Tomography: methods, history and applications*. Philadelphia: Institute of Physics Pub. 2005.
3. Putensen C., Wrigge H., Zinserling J.. Electrical impedance tomography guided ventilation therapy *Curr Opin Crit Care.* 2007;13:344-350.
4. Adler A., Amato M.B., Arnold J.H., et al. Whither lung EIT: Where are we, where do we want to go and what do we need to get there? *Physiol Meas.* 2012;33:679-694.
5. Frerichs I., Hahn G., Golisch W., Kurpitz M., Burchardi H., Hellige G.. Monitoring perioperative changes in distribution of pulmonary ventilation by functional electrical impedance tomography *Acta Anaesthesiol Scand.* 1998;42:721-726.
6. Frerichs I., Dargaville P.A., Van Genderingen H., Morel D.R., Rimensberger P.C.. Lung volume recruitment after surfactant administration

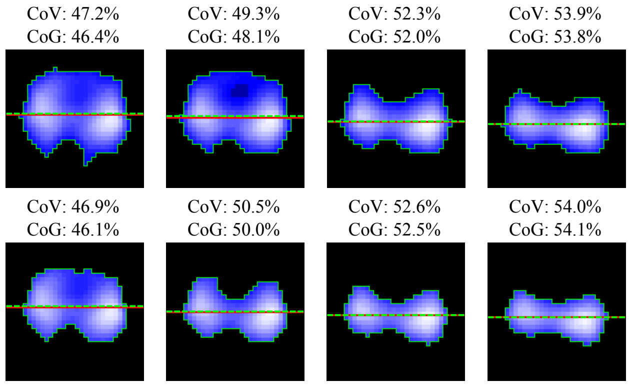

Fig. 4: The effect of PEEP and lung segmentation upon mean tidal variation (TV) images. Distribution of ventilation at four PEEP levels (from left to right, 5 to 20 cmH_2O with a step of 5 cmH_2O). Top row: thresholding set to 20% of maximum SD, bottom row: threshold set to 35% of maximum SD. The position of Center of Ventilation (CoV) and Center of Gravity (CoG) is depicted with red solid line and green dashed line, respectively. The pixel values of the image were obtained as a mean of 30 consecutive TV images.

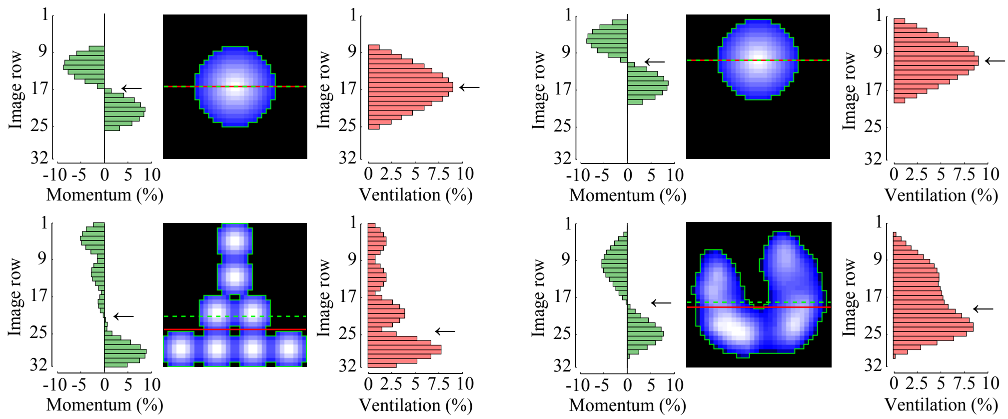

Fig. 5: The position of Center of Ventilation (CoV) and Center of Gravity (CoG) for the image structures that are symmetrical (top row) and asymmetrical (bottom row) along vertical axis. For each image, the left bar graph represents the distribution of momentum (weighted means) along vertical axis and the right bar graph shows the row sums in the normalized tidal variation (TV) image. The right bottom image is an example of TV image obtained in a spontaneously breathing healthy volunteer. The position of CoV and CoG is depicted with red solid line and green dashed line, respectively.

modifies spatial distribution of ventilation *Am J Respir Crit Care Med.* 2006;174:772-779.

7. Schibler A., Yuill M., Parsley C., Pham T., Gilshenan K., Dakin C.. Regional ventilation distribution in non-sedated spontaneously breathing newborns and adults is not different *Pediatr Pulmonol.* 2009;44:851-858.
8. Van Heerde M., Roubik K., Kopelent V., Kneyber M.C.J., Markhorst D.G.. Spontaneous breathing during high-frequency oscillatory ventilation improves regional lung characteristics in experimental lung injury *Acta Anaesthesiol Scand.* 2010;54:1248-1256.
9. Radke O.C., Schneider T., Heller A.R., Koch T.. Spontaneous breathing during general anesthesia prevents the ventral redistribution of ventilation as detected by electrical impedance tomography: A randomized trial *Anesthesiology.* 2012;116:1227-1234.
10. Blankman P., Hasan D., Erik G.J., Gommers D.. Detection of 'best' positive end-expiratory pressure derived from electrical impedance tomography parameters during a decremental positive end-expiratory pressure trial *Crit Care.* 2014;18.
11. Zhao Z., Frerichs I., Pulletz S., Müller-Lisse U., Möller K.. The influence of image reconstruction algorithms on linear thorax EIT image analysis of ventilation *Physiol Meas.* 2014;35:1083-1093.
12. Schaefer M.S., Wania V., Bastin B., et al. Electrical impedance tomography during major open upper abdominal surgery: A pilot-study *BMC Anesthesiol.* 2014;14.
13. Luepschen H., Meier T., Grossherr M., Leibecke T., Karsten J., Leonhardt S.. Protective ventilation using electrical impedance tomography *Physiol Meas.* 2007;28:S247-S260.
14. Pulletz S., Van Genderingen H.R., Schmitz G., et al. Comparison of different methods to define regions of interest for evaluation of regional lung ventilation by EIT *Physiol Meas.* 2006;27:S115.

Author: Vladimir Sobota
Institute: Faculty of Biomedical Engineering,
Czech Technical University in Prague
Street: Sitna Sq. 3105
City: Kladno
Country: Czech Republic
Email: vladimir.sobota@fbmi.cvut.cz

Sobota, V. and Roubik, K., 2016. Center of Ventilation—Methods of Calculation Using Electrical Impedance Tomography and the Influence of Image Segmentation. In *XIV Mediterranean Conference on Medical and Biological Engineering and Computing 2016* (pp. 1258-1269). Springer, Cham.